*Tectonophysics*, 133 (1987) 175–187
Elsevier Science Publishers B.V., Amsterdam – Printed in The Netherlands



# Spectral analysis of topography and gravity in the Basin and Range Province

Y. RICARD [1], C. FROIDEVAUX [1] and R. SIMPSON [2]

[1] *Laboratoire de Géophysique, Université de Paris-Sud, bat. 510, 91405 Orsay (France)*
[2] *U.S. Geological Survey, Menlo Park, CA 94025 (U.S.A.)*

(Received January 15, 1986, accepted July 23, 1986)

## Abstract

Ricard, Y., Froidevaux, C. and Simpson, R., 1987. Spectral analysis of topography and gravity in the Basin and Range Province. In: C. Froidevaux and Tan Tjong Kie (Editors), Deep Internal Processes and Continental Rifting. *Tectonophysics*, 133: 175–187.

A two-dimensional spectral analysis has been carried out for the topography and the Bouguer gravity anomaly of the Basin and Range Province in western North America. The aim was to investigate the possible presence of dominant wavelengths in the deformation pattern at the surface and at the depth of compensation. The results suggest that a 200-km wavelength in the deep compensating mass distribution has been inherited from an early tectonic phase of extension at an azimuth N65°E. The corresponding surface topography exhibits prominent overtones at wavelength of 100, 75, and possibly 45 km. It is argued that these characterize the non-linear rheology of the upper crust. The short wavelengths in the topography reflect the present phase of deformation, mixed with the results of the older deformations. These results point to a need to extend the physical models of lithospheric stretching beyond the presently available one-phase scenario. However, they show that the boudinage instability concept is consistent with the data.

## Introduction

The Basin and Range Province in western North America has experienced two successive phases of extensional tectonics during the last 40 Ma. Both followed the Laramide compression which was still active in the early Tertiary. During the first phase, subduction was widespread on the western continental edge, and the extension occurred in a SW–NE direction, somewhat perpendicular to the trench axis. For the present phase, since 15 Ma, the extension rotated to an azimuth of WNW–ESE (Zoback and Thompson, 1978) and its magnitude is of the order of 20% (Stewart, 1978). The most striking feature of the present-day topography is the regular spacing of the individual basins and ranges. This spacing defines a wavelength of about 30–50 km. A longer wavelength of about 200 km dominates the Bouguer gravity anomaly pattern between the Sierra Nevada and The Colorado Plateau. It is also present in the topography, and perhaps in the tilt domains defined by families of normal faults with the same polarity (Stewart, 1978).

This situation has prompted us to carry out a careful spectral analysis of the topography and gravity data set restricted to the Basin and Range Province alone. The same data set was used by U.S.G.S. workers to produce global U.S. filtered maps separating short and long wavelengths (Hildenbrand et al., 1982). By using only one given tectonic region we hope to better resolve the characteristic periodicities with their wavelengths and azimuths. The high density of measured grav-

0040-1951/87/$03.50 

ity values favors a reliable numerical analysis, whereas the apparent uniformity of the tectonic style gave the expectation of meaningful results. One further ingredient to be weighted in interpretations is the observation by COCORP of rather flat Moho and lower crust reflectors (Allmendinger et al., 1986). This type of horizontally layered deep structure also characterizes other subsiding provinces, as in northern France (Bois et al., 1985) and in the Celtic Sea (BIRPS and ECORS, 1986)

Two kinds of tectonic models have been proposed for the Basin and Range Province. In the first, geometric crustal cross-sections are given that describe the décollement horizons and the normal faults, with some indication of the possible kinematic history (Stewart, 1978; Wernicke, 1981; Brun and Choukroune, 1983). Such structural models are not intented to account for the existing periodicities in physical terms. The origin of these periodicities constitutes the starting point of the second kind of models. In such models one faces the difficulty of formulating a rheological behavior in which faults can be generated. Therefore, up to now, such models have been based on continuous rheologies, e.g., non-linear viscous or plastic. They yield some large-scale characteristics of the deformation patterns such as the wavelength and growth rate of folding or boudinage. This last mechanism was proposed to explain the 30–50 km wavelength of the Basin and Range topography (Fletcher and Hallet, 1983). Here stretching instabilities of the competent seismic crust resting upon a weak ductile lower crust lead to the formation of pinches and swells, which explain the observed topography. A similar mechanism could apply to the mantle lithosphere which forms a second competent layer. Because of its larger thickness, this second layer could yield a larger boudinage wavelength, say 200 km (Froidevaux and Ricard, 1985; Froidevaux, 1986). Such proposals have encouraged the investigation of stretching instabilities in stratified lithospheric structures with realistic geometries and rheologies (Ricard and Froidevaux, 1986; Zuber et al., 1986). These theoretical studies have established the possible existence of modes of deformation with preferred wavelengths controlled by the thickness of the layers. Overtones of these modes are predicted when the rheology of the competent layers is close to perfect plasticity. The spectral analysis undertaken here may thus also throw some light on the large-scale mechanical behavior of the Earth's lithosphere.

**Data set and method of analysis**

The gravity data set was that used to prepare the Gravity Anomaly Map of the United States (Society of Exploration Geophysicists, 1982). It is based on one million on land gravity measurements with a typical density of 10 points in a 10 by 10 km square. Interpolated values were defined on a regular grid with a 4 km mesh (Godson and Scheibe, 1982). Topography data used here were 3-minute data which were regridded to a 4 km mesh grid coincident with the gravity data. These data grids are the starting point of our numerical analysis. Fig. 1 is an index map of the region under consideration. The two squares define the regions chosen for our data analysis. Plate I contains two maps constructed with our data using an Albers equal area projection. Each map is a 800 × 800 km square. It corresponds to the larger square on Fig. 1. It covers part of southern California with Los Angeles near the southwestern corner and includes the striking contrast between Great Valley and Sierra Nevada. This contrast is marked by the transition from green to red seen in Plate Ia, which depicts the topography. To the east of this mountain range lies the Basin and Range Province across the State of Nevada and into Utah. Salt Lake City is located near the northeastern corner in the yellow area of Plate Ia. The Wasatch mountains along the eastern edge of this map mark the edge of the Colorado Plateau. These structures also appear distinctly on the Bouguer anomaly map of Plate Ib. As noticed by earlier authors (Eaton et al., 1978) two marked gravity Bouguer minima lie over the Basin and Range. This could reflect some deep compensation rather than density variations near the surface. This opinion derives from the absence of any obvious correlation with the pattern of geological terrains.

A two-dimensional Fourier analysis was carried out within the domain D of the above maps. Each data set defined as a function $f(x, y)$ is trans-

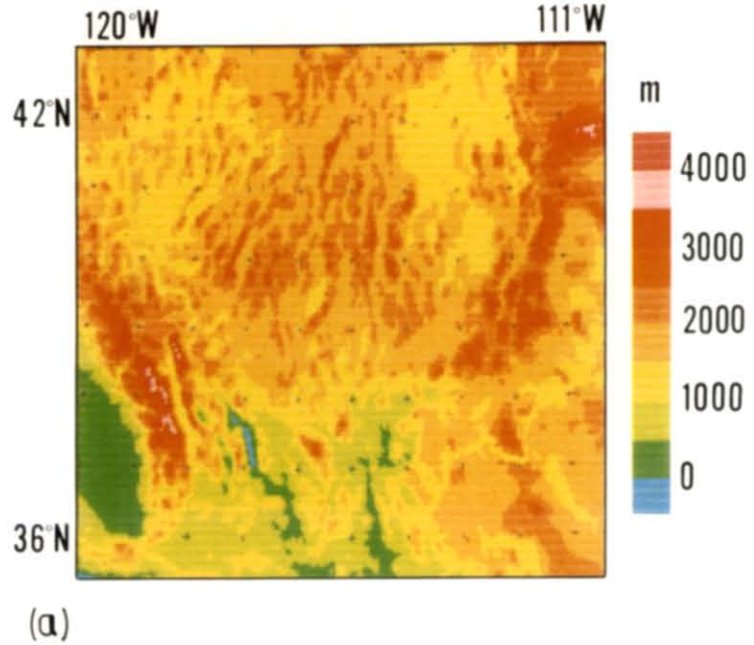


PLATE I

Topography (a) and Bouguer gravity anomaly (b) maps of the Basin and Range Province. The geographical coordinates are given near the edges and indicated by crosses inside the domain. In this equal area Albers projection the great and small circles are not parallel to the edges. These maps cover 800 × 800 km corresponding to the large square in Fig. 1.

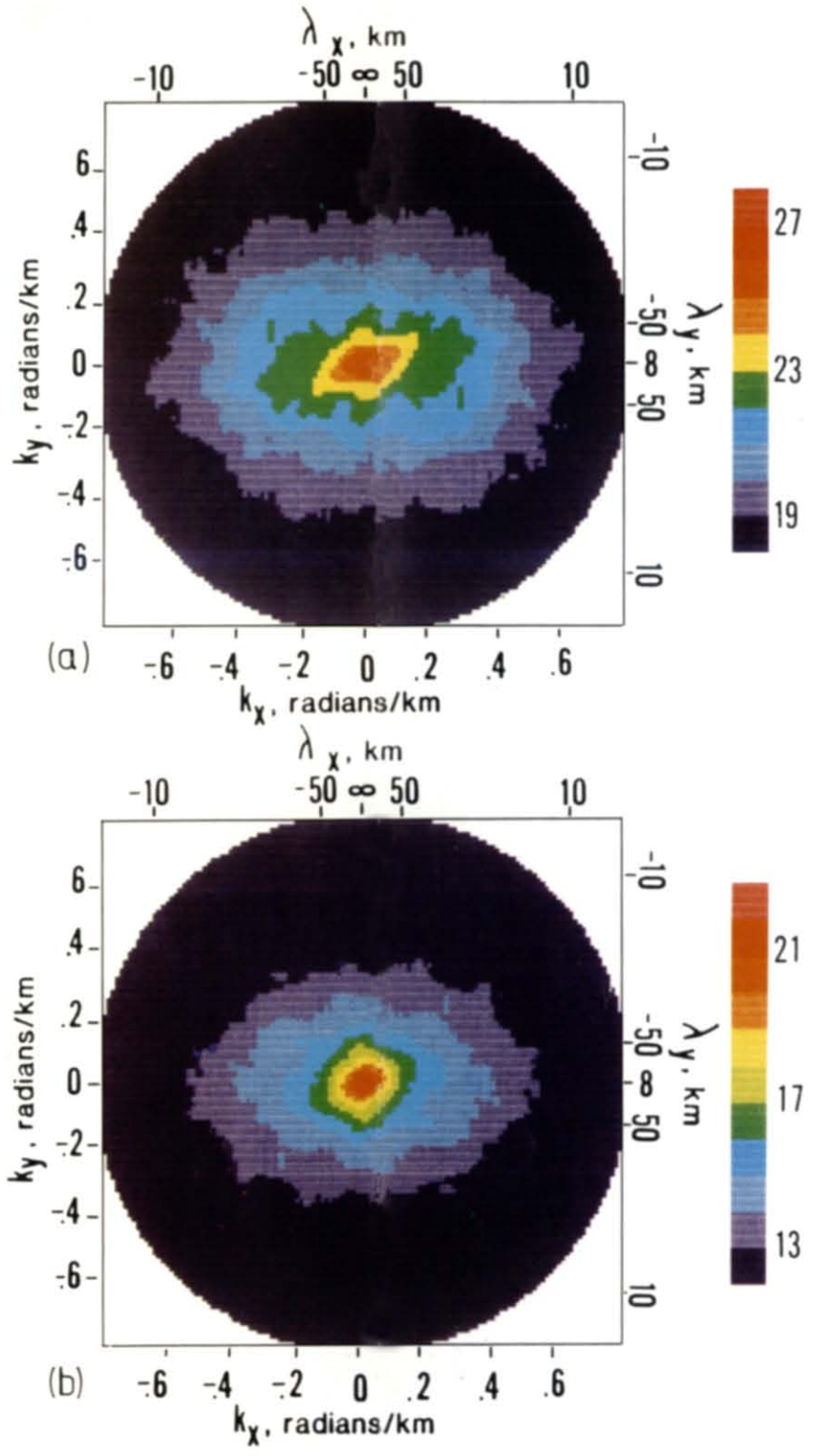


PLATE II

Total power spectra for topography (a) and Bouguer gravity anomaly (b) of the domain defined by the maps in Plate I. These spectra are plotted vs. a linear scale in wavenumbers $k_x$ and $k_y$. The equivalent wavelength values are also given. The amplitudes depicted by the color code are defined by eqn. (3).

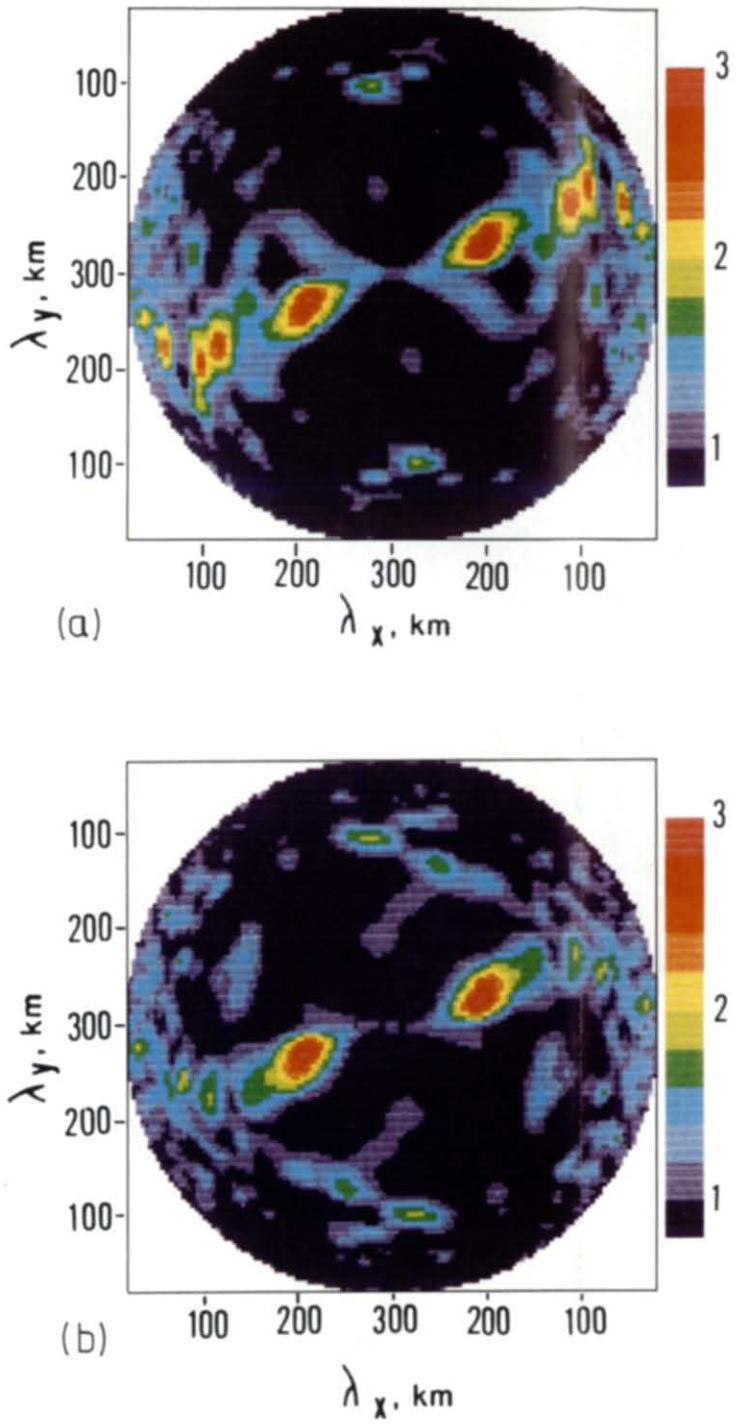


PLATE III

Non-isotropic part of the Fourier amplitudes corresponding to the domains defined by the maps of Plate I. This function for topography (a) and Bouguer (b) is normalized, i.e. amplitudes given by the color scale are expressed in terms of the average value within a ring of radius $k = 2\pi/\lambda$. The coordinate system of this Figure is linear in wavelengths $\lambda_x$ and $\lambda_y$. It spans the values from 20 km at the edge of the colored area to 300 km at the center.

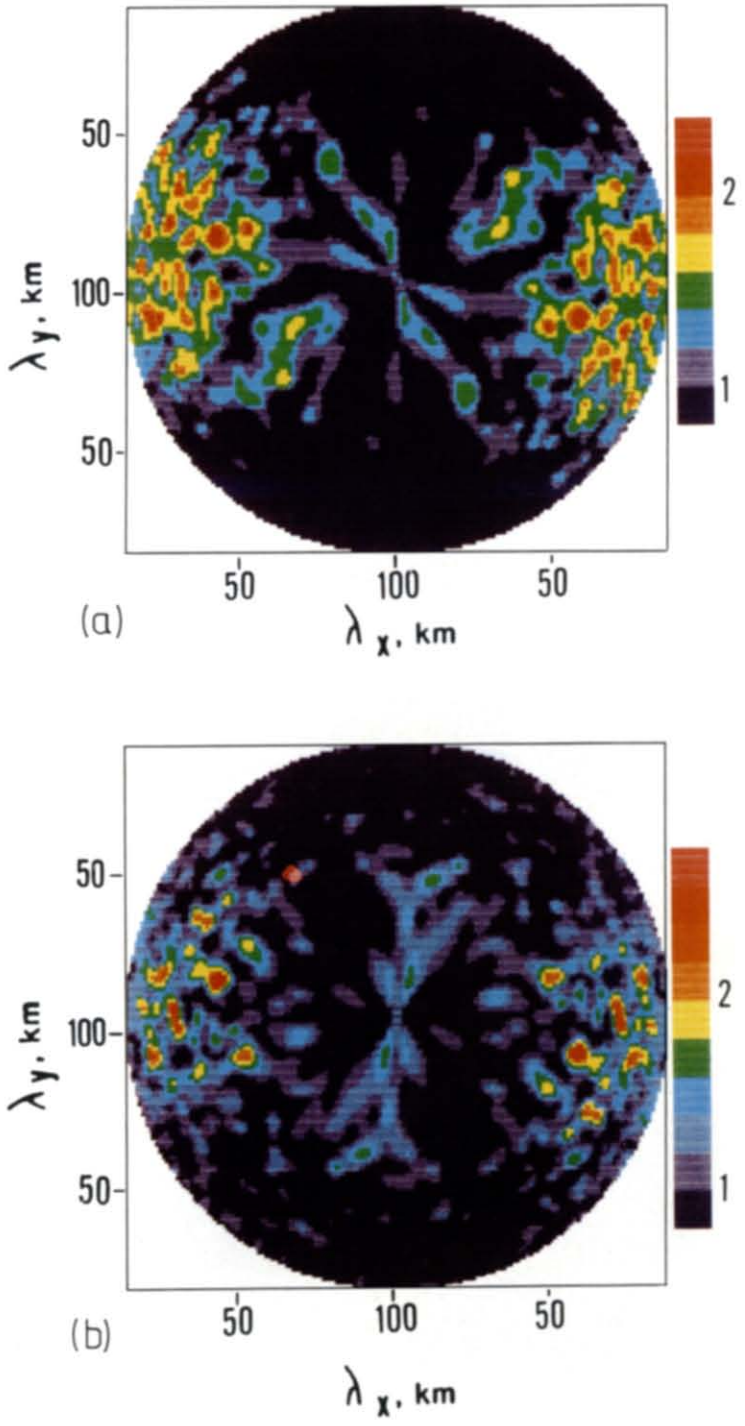


PLATE IV

Non-isotropic part of the Fourier amplitudes vs. wavelengths $\lambda_x$ and $\lambda_y$. This representation is similar to that of Plate III, but here the square domain where the topography and Bouguer anomaly were Fourier analyzed is only 640 × 640 km as shown by the small square in Fig. 1. The computed spectra are plotted for a range of wavelengths between 20 and 100 km.

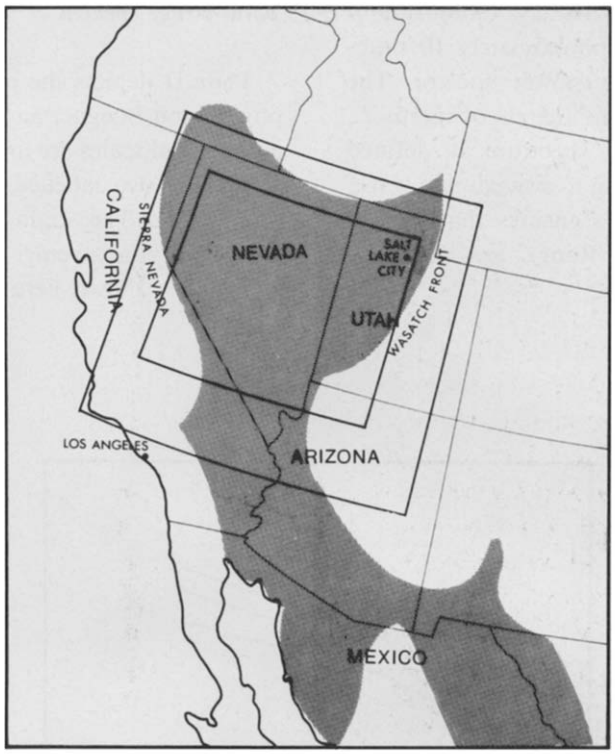


Fig. 1. Index map of the western North America. The squares correspond to the areas under study in this paper. The shaded area shows the Basin and Range Province.

formed into $F(k_x, k_y)$, a function in the wavevector domain:

$$F(k_x, k_y) = \iint_D f(x, y)\, e^{i(k_x x + k_y y)}\, dx\, dy \qquad (1)$$

Here the wavevector $\boldsymbol{k}$ with components $k_x$ and $k_y$ defines a wavelength $\lambda$ according to:

$$\lambda = \frac{2\pi}{\sqrt{k_x^2 + k_y^2}} \qquad (2)$$

The above function $F(k_x, k_y)$ is complex-valued and one usually defines a real quantity $A$ which is the logarithm of the power spectrum given by:

$$A(k_x, k_y) = \ln |F(k_x, k_y)|^2 \qquad (3)$$

The Fourier transform of a sinusoidal undulation generates two peaks in the power spectrum. These peaks are symmetrically located at a distance $|\boldsymbol{k}|$ from the origin. They lie at an azimuth perpendicular to the crests and troughs of the sinusoidal undulation.

Because the starting data is specified on a grid, the above integrals must be replaced by discrete summations. As a consequence the Fourier wavenumber domain is also defined on a grid with mesh $\Delta k = 2\pi/L$, where $L$ is the dimension of the sampling area. This grid has the same number of nodes as the data grid of mesh $\Delta l$. It covers a domain where both $k_x$ and $k_y$ are smaller than $\pi/\Delta l$. In this study one has $L = 800$ km and $\Delta l = 4$ km. Thus the computed power spectra are defined for wavelengths between 8 and 800 km in the E–W and N–S directions.

Technical tests with different values for the size $L$ of the data domain and the mesh $\Delta l$ of the grid have been carried out. They did show that our results are quite insensitive to such changes. Another problem arises because of edge effects. Indeed the discontinuity of the analyzed function $f(x, y)$ on the sides of its domain can artificially reinforce the power spectrum along the grid axes. A simple procedure was set up to reduce this well

known artifact (Ricard and Blakely, 1986). It consists of rotating the grid approximately 10 times and stacking the resulting power spectra. The analyzed domain is therefore a circle of radius $L$, and the computed power spectrum is defined within a circle corresponding to a maximum wavelength $\lambda = L$. This methods ensures that our results for the Basin and Range are not contaminated with edge effects.

**Total power spectra**

Plate II depicts the power spectra for topography (a) and Bouguer anomalies (b). The horizontal and vertical scales are linear in wavenumber. These scales are also labelled in wavelength between 8 and 800 km. The origin $k = 0$ ($\lambda = \infty$) only corresponds to the average value of the data. The amplitudes shown here are slightly smoothed. A

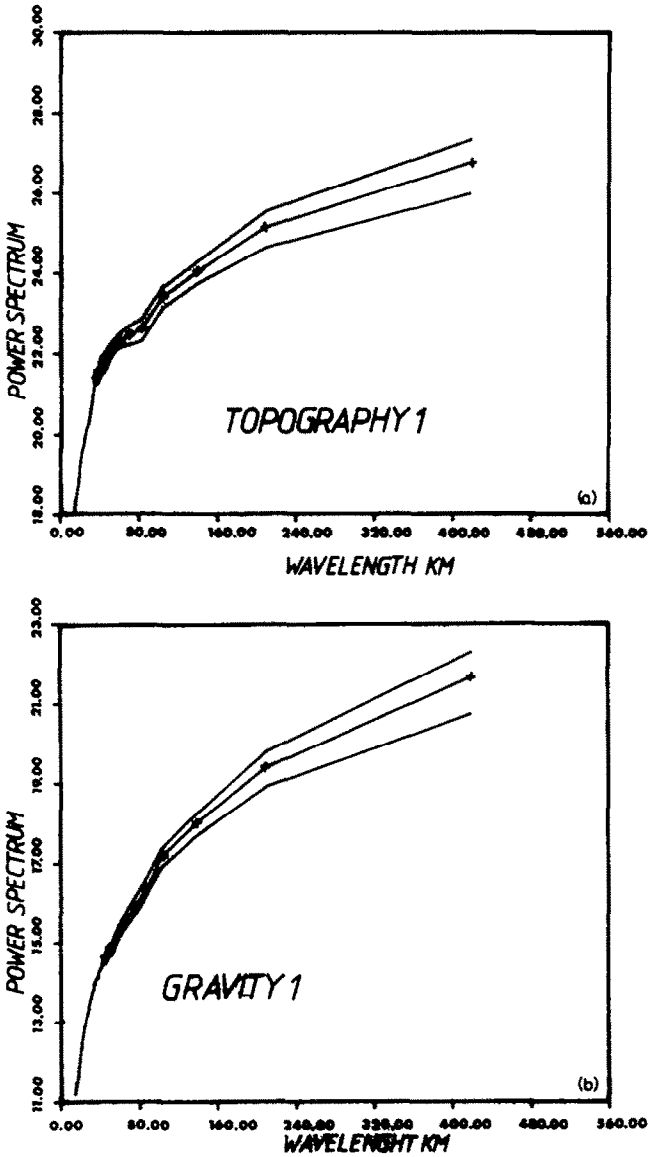


Fig. 2. Mean values of the power spectra amplitudes of Plate IIa, b vs. wavelength averaged around concentric rings in the wavenumber $k$ plane. The upper and lower curves define the amplitude of the variance.

$5 \times 5$ mesh averaging window is moved over the $200 \times 200$ mesh domain. Two features are especially apparent. One is the dramatic decrease in amplitude towards the edges of the plot (large $k$ values). The other is the overal E–W ellipticity of these patterns. The sharp decrease means that the most significant structures occur for wavelengths larger than a certain threshold. The latter amounts to some 30 km in the case of the topography, if one defines it by a drop of six units, i.e. by an amplitude reduction of 1000. In Plate IIa this threshold is at the outer edge of the green area. For gravity, in Plate IIb, it is about twice as large and lies at the boundary between pale and dark green. The most meaningful information is thus concentrated near the center of these color plots. If one now restricts our attention to the ellipticity in this area, one notices that it shows up particularly strongly for the topography. This corresponds to the fact that the structures strike mostly N–S.

In the next section the long wavelength portion of the power spectra will be expanded and looked at in more detail. To achieve this, these spectra will be split into their isotropic and anisotropic components, a procedure also used at larger scale (Simpson et al., 1986). Figure 2 depicts the averaged values $\langle A \rangle$ with respect to the wavelength. This represents the mean value within a ring of mean radius $\langle k \rangle = 2\pi/\lambda$. This isotropic component shows little structure. In particular no peak is found near 200 km, and the weak deflection around 50 km in the topography plot of Fig. 2a is not really convincing. Obviously the most instructive signal must be hidden in the azimuthally dependent component.

**Dominant periodicities**

Fourier transform values $F(k_x, k_y)$ calculated to build the smoothed power spectra of Plate II were used in their rough shapes in order to examine their possible fine structure. In order to enhance the non-isotropic part of the spectra, an average value $\langle |F(|k|)|^2 \rangle$ was computed in the same manner as $\langle A \rangle$ shown in Fig. 2. The anisotropic component equal to $|F(k_x, k_y)|^2 / \langle |F(|k|)|^2 \rangle$ was then plotted in two dimensions as a function of wavelength in Plate III. When transformed to the wavelength domain the grid becomes non-uniform. A continuous representation was derived by linear interpolations. The scarcity of grid points at wavelengths close to the dimension of the sampling domain has led us to restrict our plots to a domain with $20 < \lambda < 300$ km.

Both topography and gravity spectra treated in this manner yield anisotropic components with marked peaks illustrated by the red dots of Plate IIIa, b. There the amplitude of the maxima is about three times the mean value for the same wavelength. These peaks define an azimuth N65°E. For smaller wavelengths, peaks tend to have an azimuth more in an E–W orientation as seen in particular for the topography which exhibits stronger peaks. These were looked at in more detail by Fourier analyzing a restricted area which excludes the periphery of the maps of Plate I to avoid possible contaminations from outside the Basin and Range. This new $640 \times 640$ km domain, shown in Fig. 1, of course yields less information at large wavelength, but the new results still agree with the previous ones. Plate IV depicts the short wavelength peaks for $20 < \lambda < 100$ km. Again they are more marked for the topography. Interestingly, they cluster around an azimuth N100°E.

The red peaks in Plate IIIa correspond to wavelengths of 200, 100, 75 and 45 km respectively. The breadth of these peaks indicates that the above values have about 10% accuracy. They might be considered as one fundamental mode at 200 km with three overtones at wavelengths close to the ratio 1/2, 1/3 and 1/4. For gravity only the fundamental at 200 km is clearly defined.

**Interpretation and conclusion**

The change in azimuth from N65°E for the large wavelength peaks of Plate III to N100°E for the short wavelength cluster of Plate IV happens to correlate with the change of orientation of the extensional stress $\sigma_3$ recorded around 15 Ma (Zoback and Thompson, 1978). The dominant 200 km wavelength anomaly present in the Bouguer map may thus correspond to deep structures de-

veloped during the initial phase of Basin and Range tectonics. If so this compensating structure apparently still prevails. The filtered Bouguer maps (Hildenbrand et al., 1982; Froidevaux, 1986) reveal the penetration of this structure into the southern part of the province, i.e. in the State of Arizona. This also applies to the topography. The second phase of extension, which spans the last 15 Ma, has apparently reoriented the short wavelength topography, as shown by our data analysis. This last deduction confirms numerous geological observations (Eaton et al., 1978; Zoback and Thompson, 1978). The wide distribution of the 20–50 km wavelength peaks on Plate IVa may illustrate the coexistence of old and new trends. One should emphasize that there are no long wavelength peaks at the correct azimuth to correspond to the presently active deformation. However there is a weak N–S pair of peaks with wavelength 100 km in Plate III; their tectonic significance is not clear to us.

The above demonstration of a superposition of two distinct modes of lithospheric deformation induces us to make some comments on recently proposed mechanical models for the Basin and Range (Froidevaux, 1986; Zuber et al., 1986). These models invoke the generation of stretching instabilities leading to a boudinage of a rheologically layered lithosphere. Possible simultaneous double wavelength modes are proposed for a single extensional phase. Our present analysis shows the necessity to treat the problem as time-dependent and three-dimensional. Our discussion suggests that the early structures must have been reactivated by the recent stress field. This would imply a mixture of normal and dextral strike-slip components in the present tectonic style.

The occurrence of overtones in the normalized topography spectrum of Plate IIIa and their absence in the Bouguer spectrum of Plate IIIb probably reveals differences in rheological behavior between upper and deeper parts of the lithosphere. Strong overtones of the 200 km wavelength fundamental indicate that the deformation is not sinusoidal, but concentrated in narrower zones. The brittleness of the upper crust is obviously responsible for this (Ricard and Froidevaux, 1986). The possible deep compensating structures revealed by the normalized Bouguer spectrum appear to be smoother as indicated by the absence of overtones. This must reflect a smaller degree of non-linearity of the ductile mantle lithosphere. The flatness of the Moho structures shown by the COCORP profiles suggests that compensation is at least partly thermal and below the Moho (Froidevaux, 1986).

Marginal stability analysis of stretching does indeed predict overtones of the fundamental boudinage mode (Ricard and Froidevaux, 1986). However, these models only yield odd harmonics. In the light of this, the observed 200, 100, 75 and 45 km modes should rather be interpreted as overtones number 3, 5, 7 and 9. The fundamental would thus correspond to a wavelength equal to the whole width of the Province, about 550 km.

One could raise the question of why the present spectral analysis of topography and gravity has not been carried one step further by presenting the admittance curve for the Basin and Range Province. This function has indeed been computed, but the limited size of our domain does not yield much new physical insight. Such an analysis has already been undertaken (McNutt, 1980) for the western U.S.A. and showed a vanishing elastic thickness for the lithosphere. The two-dimensional admittance function we computed turned out to be strongly anisotropic, as can be expected from the details of Plate III. Up to now, all workers have restricted their considerations to one-dimensional admittance functions. These are obtained by making averages for a given value of $|k|$, as was done here for the power spectra in Fig. 2. Implicitly, these authors treat the anisotropic components as noise. Our case study has shown that the anisotropy can be physically meaningful and connected with the trends of tectonic structures and with their possible evolution in time.

**Acknowledgement**

This work was carried out with the partial support of the French Center for Space Research (CNES).

**References**

Allmendinger, R.W., Hauge, T., Hauser, E.C., Potter, C. and Oliver, J., 1986. Tectonic heredity and the layered lower

crust in the Basin and Range Province, western United States. J. Geol. Soc. of London, in press.

BIRPS and ECORS, 1986. Deep seismic reflexion profiling between England, France and Ireland. J. Geol. Soc. of London, in press.

Bois, C., Damotte, B., Mascle, A., Cazes, M., Torreilles, G., Galdéano, A., Hirn, A., Matte, P. and Raoult, J.P., 1985. Deep seismic profiling of the crust in northern France: the ECORS. In: M. Barazangi and L. Brown (Editors), Deep Structure of Continental Crust. Geodyn. Ser., Vol. 13. Am. Geophys. Union, Washington, D.C., pp. 21–30.

Brun J.P. and Choukroune, P., 1983. Normal faulting, block tilting and décollement in a stretched crust. Tectonics, 2: 345–356.

Eaton, G.P., Wahl, R.R., Prostka, H.J., Mabey, D.R. and Kleinkopf, M.D., 1978. Regional gravity and tectonic patterns: their relation to late Cenozoic epeirogeny and lateral spreading in the western Cordillera. In: R.B. Smith and G.B. Eaton (Editors), Cenozoic Tectonics and Regional Geophysics of the Western Cordillera. Geol. Soc. Am., Mem., 152: 51–59.

Fletcher, R.C. and Hallet, B., 1983. Unstable extension of the lithosphere: a mechanical model for Basin and Range structure. J. Geophys. Res., 88: 7457–7466.

Froidevaux, C. and Ricard, Y., 1985. Lithospheric tectonics in the Basin and Range Province. Terra Cognita, 5: 307.

Froidevaux, C., 1986. Basin and Range large scale tectonics: constraints from gravity and reflection seismology. J. Geophys. Res., 91: 3625–3632.

Godson, R.H. and Scheibe, D.M., 1982. Description of magnetic tape containing conterminous U.S. gravity data in gridded format. U.S. Dep. Commer., Natl. Tech. Info. Serv., PB82-254798 (magnetic tape with description), 5 pp.

Hildenbrand, T.G., Simpson, R.W., Godson, R.H. and Kane, M.F., 1982. Digital colored residual and regional Bouguer gravity maps of the conterminous United States with cut-off wavelengths of 250 km and 1000 km. U.S. Geol. Surv. Geophys. Invest., map GP-953-A, scale 1 : 7,500,000.

McNutt, M.K., 1980. Implications of regional gravity for the state of stress of the earth's crust and upper mantle. J. Geophys. Res., 85: 6377–6396.

Ricard, Y. and Blakely, R., 1986. A new method to minimize edge effects in 2D Fourier transform. Geophysics (submitted).

Ricard, Y. and Froidevaux, C., 1986. Stretching instabilities and lithospheric boudinage. J. Geophys. Res , 91: 8314–8324.

Simpson, R.W., Jachens, R.C., Blakely, R.J. and Saltus, R.W., 1986. A new isostatic residual gravity map of the conterminous United States with a discussion on the significance of isostatic residual anomalies. J. Geophys. Res., 91: 8348–8372.

Society of Exploration Geophysics, 1982. Gravity anomaly map of the United States. Soc. Explor. Geophysicists, scale 1 : 2,500,000.

Stewart, J.H., 1978. Basin and Range structure in western North America: a review. In: R.B. Smith and E.P. Eaton (Editors), Cenozoic Tectonics and Regional Geophysics of the Western Cordillera. Mem. Geol. Soc. Am., 152: 1–32.

Wernicke, B., 1981. Low-angle normal faults in the Basin and Range Province: nappe tectonics in an extending orogen. Nature, 291: 645–648.

Zoback, M.L. and Thompson, G., 1978. Basin and Range rifting in northern Nevada: clues from a mid-Miocene rift and its subsequent offsets. Geology, 6: 111–116.

Zuber, M.T., Parmentier, E.M. and Fletcher, R.C., 1986. Extension of continental lithosphere: a model for two scales of Basin and Range deformation. J. Geophys. Res., 91: 4826–4838.